Anti-reflective Microengineered Substrate for in vitro Ultrasound Neuromodulation

Wardhana, Gandhika K.; Costa, Tiago L.; Mastrangeli, Massimo

DOI
10.1109/UFFC-JS60046.2024.10793577

Publication date
2024

Document Version
Final published version

Published in
IEEE Ultrasonics, Ferroelectrics, and Frequency Control Joint Symposium, UFFC-JS 2024 - Proceedings

Anti-reflective Microengineered Substrate for *in vitro* Ultrasound Neuromodulation

Gandhika K. Wardhana
Microelectronics Department
Delft University oftechnology
Delft, the Netherlands
G.K.Wardhana@tudelft.nl

Tiago L. Costa
Microelectronics Department
Delft University oftechnology
Delft, the Netherlands
T.M.L.daCosta@tudelft.nl

Massimo Mastrangeli
Microelectronics Department
Delft University oftechnology
Delft, the Netherlands
M.Mastrangeli@tudelft.nl

2024 IEEE Ultrasonics, Ferroelectrics, and Frequency Control Joint Symposium (UFFC-JS) | 979-8-3503-7190-1/24/$31.00 ©2024 IEEE | DOI: 10.1109/UFFC-JS60046.2024.10793577

***Abstract*—Poor stimulus-response correlation, caused by acoustic reflections from conventional culture substrates, poses a significant challenge in cellular mechanistic studies of ultrasound neuromodulation. Existing specialized setups that mitigate this interference have limited recording capabilities. In this study, we propose an anti-reflective microengineered substrate (ARMS) that can be incorporated into a standard *in vitro* platform. The substrate's dimensions and material composition were optimized in simulation. The optimized simulated platform exhibited an 86.3% reduction in reflection amplitude on the substrate surface compared to the conventional glass substrate. Furthermore, the ARMS reduced stimulation signal distortion to a 19.2% deviation from the expected amplitude, a substantial improvement compared to the 76.4% deviation observed with glass.**

Index Terms*—anti-reflection, neuromodulation, *in vitro

I. Introduction

In vitro models are crucial for drug development, particularly for screening, safety assessment, as well as for mechanistic studies. In this respect, the mechanisms of ultrasound neuromodulation and the influence of different ultrasound parameters on neuronal excitation or inhibition remain poorly understood [1]. *In vitro* models offer a controlled environment to study these cellular mechanisms, mitigating the confounding effects of anesthesia often present in animal models [2]. Unfortunately, commercial *in vitro* platforms are typically incompatible with acoustic stimuli. The typically used glass or hard plastic material, along with their enclosed nature, lead to wave reflections that interfere with the intended stimuli, potentially causing poor stimulus-response correlations [3]. This contrasts with the open, echo-free environment used for transducer calibration.

While the distorted stimulus waveform can be predicted, for instance by using a finite element model (FEM), the distortion can be substantial, and validating the prediction is challenging [3]. Specialized setups, such as suspending mylar film on degassed water as a culture substrate, have been used to considerably reduce reflection [4]. However, this approach is not compatible with the incorporation of electrodes for electrophysiological characterization of neuronal tissue.

To address the reflection issue, we envisioned an ultrasound-compatible *in vitro* platform that minimizes acoustic reflection while maintaining compatibility with conventional formats, such as microelectrode arrays and microplates. In this study, we propose the design of an anti-reflective microengineered substrate (ARMS), as seen in Fig.1. The concept involves two polymer layers as a culture substrate placed beneath culture wells. The first layer of polymer acts as a biocompatible interface on which electrodes can be microfabricated. The second layer of polymer acts as a wave absorber. The interface between the polymers forms an array of pillars that serve as the anti-reflective structure. The structure increases the number of times a wave bounces at an interface. With each bounce, the wave is partially transmitted and reflected, dissipating its energy over time.

The work is organized as follows: Section II details the simulation setup, material selection, and assessment metrics employed in this study. Section III presents the simulation results, including the optimization of ARMS dimensions and material composition, and a comparison with conventional substrates. Section IV concludes the study, summarizing the key findings and their implications.

II. Methods

A. Simulation setup

The simulation setup implemented in the k-Wave toolbox in MATLAB is illustrated in Fig.2(b). The ARMS model comprises three main components: the ultrasound source and the first and second polymer layers. The ultrasound source was positioned at a fixed distance from the substrate, and a single ultrasound pulse was generated at a desired frequency. The optimization of ARMS will primarily focus on the 1-2 MHz range, which aligns with the ultrasound frequencies typically reported in the literature [1], [3].

ARMS performance was assessed by comparing it to two reference cases. The first reference simulation modeled the source in the absence of a substrate. This aimed to observe wave propagation from the transducer in a reflection-free environment, representing typical transducer characterization conditions. The second reference simulation modeled wave propagation in the presence of a conventional substrate, as depicted in Fig.2(a). The influence of several materials commonly used as culture substrates on wave propagation was assessed. In particular, the glass substrate was used as a reference due to its high reflection amplitude.

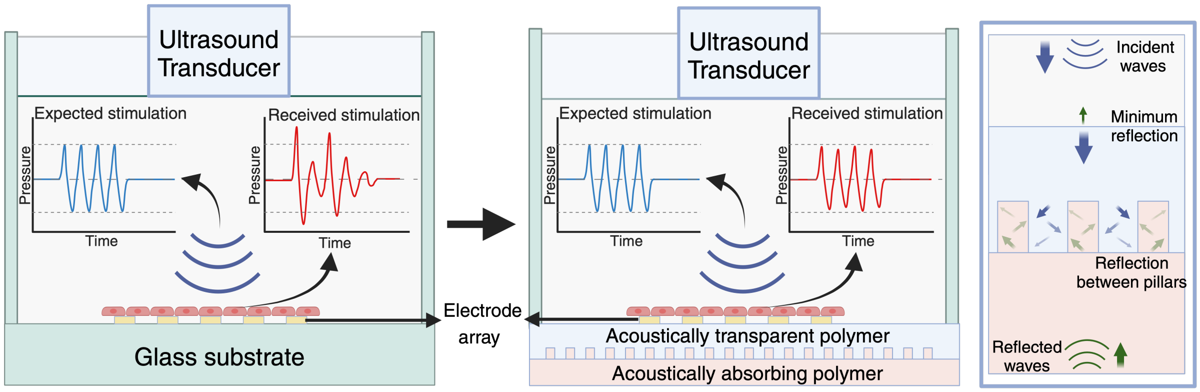

Fig. 1. A schematic showing the concept of ARMS, which can preserve stimulation fidelity, unlike a conventional glass substrate. The ARMS consists of two distinct polymer layers. The interface between the layers forms an array of pillars that maximize the occurrence of partial reflections, thereby distributing reflected energy over time.

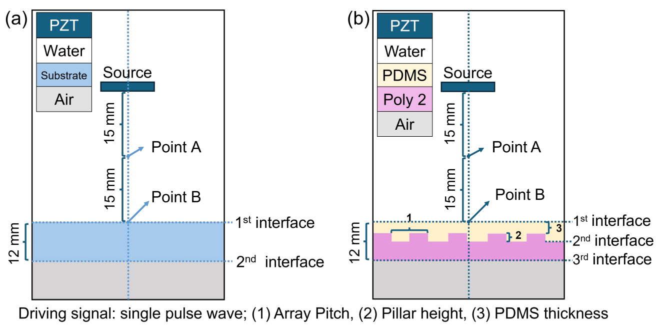

Fig. 2. Schematics of the simulation setup used in k-Wave for (a) the conventional substrates and (b) the ARMS.

TABLE I
ACOUSTIC PROPERTIES OF MATERIALS USED IN NUMERICAL SIMULATION IN K-WAVE [5].

Material	Speed of sound (m/s)	Density (kg/m^3)	Acoustic impedance $(MRayl)$
Water	1480	1000	1.48
glass	5900	2200	1.045
air [6]	331	1.225	0.0004
PDMS [7]	1077	970	1.045
Polyethylene	1950	930	1.814
Polystyrene	2320	1040	2.413
Polylactic acid	2220	1240	2.753
Epoxy [8]	2650	1150	3.05
PMMA	2757	1190	3.28
SU-8 [9]	2917	1200	3.5
Melopas	2900	1700	4.93

B. Material selection

In choosing the material for the acoustically transparent polymer, several considerations were taken into account: (1) acoustic impedance similar to water to minimize reflection, (2) biocompatibility to host cell cultures, and (3) compatibility with microfabrication processes. Polydimethylsiloxane (PDMS) is widely used in organ-on-chip and microfluidics applications [10], [11]. PDMS-based devices have moreover demonstrated biocompatibility with various cell cultures, contributing to their widespread adoption. Compatibility with microfabrication processes allows electrodes to be deposited directly onto the PDMS surface. Acoustic impedance is another crucial consideration. Since the source-facing surface of the polymer is flat to accommodate cells and electrodes, reflection is inevitable; therefore, minimizing reflection at this interface is crucial. PDMS has an acoustic impedance similar to water. The PDMS-water interface has a reflection coefficient of 0.172, significantly lower than that of Polystyrene (PS) (0.24) and glass (0.795). Due to this combination of properties, PDMS was selected as the first polymer layer. There are fewer constraints when choosing the material for the second polymer layer. As the second layer will not contact the cell culture, biocompatibility is not a constraint. Therefore, several materials with a range of acoustic properties were considered for the second polymer layer. Table I lists the properties of the materials used in the simulation, including those considered for the second polymer layer.

C. Assessment metric

Two assessment metrics were utilized: echo reduction (ER) and deviation. Echo reduction, measured at Point A (Fig.2), compares the echo amplitude of the measured configuration to that of a glass reference.

$$Echo\,reduction\,(\%) = 100\% - \left(\frac{Echo_{meas}}{Echo_{glass}}x100\%\right) \quad (1)$$

where $Echo_{meas}$ is the peak-to-peak reflection amplitude of the measured configuration, and $Echo_{glass}$ is the peak-to-peak reflection amplitude of the glass substrate. Deviation, calculated at Point B (Fig.2), quantifies the difference in peak-to-peak amplitude between the stimulation signal and the expected signal in a reflection-free environment.

$$Deviation\,(\%) = \left(\frac{|signal_{water} - signal_{meas}|}{signal_{water}}x100\%\right) \quad (2)$$

where $signal_{water}$ is the peak-to-peak amplitude of the expected stimulation signal measured in a reflection-free environment, and $signal_{meas}$ is the peak-to-peak amplitude of the measured stimulation signal.

III. Result and discussion

A. Reference measurement

A simulation of an echo-free environment was performed as a reference for the deviation, as seen in Fig.3(a). A single wave burst was observed in both Point A and B, which originated from the single pulse applied to the source. The absence of reflected waves validated the effectiveness of the perfectly matched layer implemented on the boundary of the simulation space. The amplitude of the pulse shown in Point B indicates the stimulation signal amplitude that would be applied to the stimulation target on the surface of the substrate.

Fig.3(b) and Fig.3(c) depict the time-domain observations for glass and PS substrates, respectively. Glass is commonly used as a microelectrode array substrate, while PS is the typical hard plastic material making up well-plates. Reflection is observed in the presence of both substrates. At Point A, the reflection in glass is predominantly from the first interface, while in PS, it is dominated by the second interface. Distortion of the stimulation signal is evident in both substrates. Additional echoes following the primary stimulation wave are also observed in both substrates. Notably, the glass substrate exhibits a particularly pronounced 76.4% increase from the expected signal amplitude.

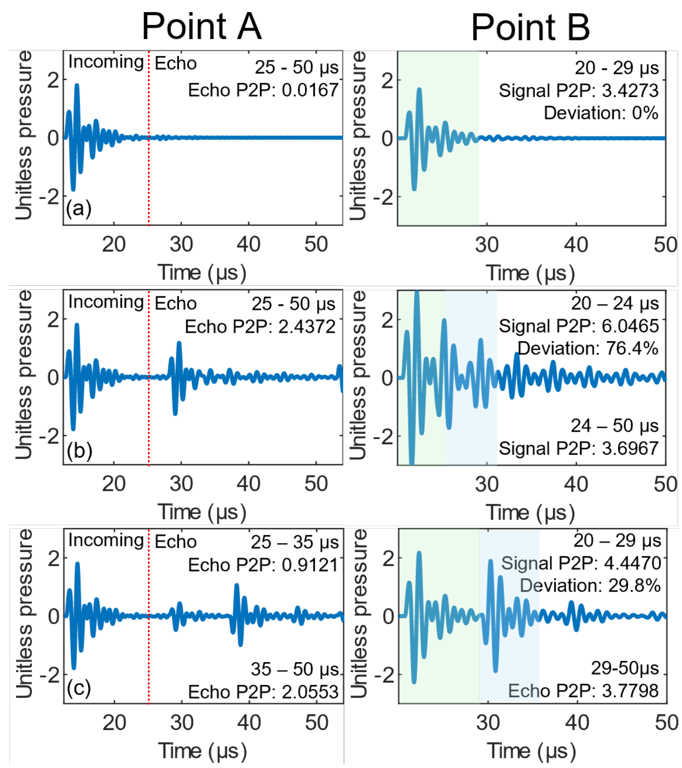

Fig. 3. Timed-domain simulation result at Point A and B: (a) echo-free condition mimicking the typical condition of ultrasound characterization. (b) the same transducer with glass substrate placed on the front of the transducer. (c) the same transducer with Polysytrene substrate placed on the front of the transducer.

B. Optimization

Optimization of PDMS thickness, array pitch, and height was performed on the ARMS. Optimization was conducted by holding other parameters constant and varying one parameter at a time. Polymethyl methacrylate (PMMA) was used as the absorbing polymer. The echo reduction at Point A served as the comparison metric during optimization. During the optimization of PDMS thickness (Fig.4(a)), the pillar pitch and height were fixed at 10 mm and 2 mm, respectively. It was observed that the thickness of PDMS above the pillar array did not influence ARMS performance. Next, the array pitch was optimized while keeping the PDMS thickness constant at 2 mm and 5 mm (Fig.4(b)). The pitch significantly affected ARMS performance. At both 1 MHz and 2 MHz ultrasound frequencies, ARMS performance decreased significantly at pitches below 2 mm and above 10 mm. The optimal pitch was determined to be 10 mm. Subsequently, pillar height optimization was performed with the array pitch and PDMS thickness held constant at 10 mm and 5 mm, respectively (Fig.4(c)). A positive correlation was found between echo reduction and pillar height, likely due to the increased number of reflections caused by taller pillars. This correlation was more pronounced at 1 MHz than at 2 MHz. The optimal pillar height was 4 mm for 1 MHz and 6 mm for 2 MHz. Finally, optimization of material combinations was conducted using several polymers with acoustic impedances ranging from 1.8 MRayl to 4.9 MRayl. As shown in Fig. 5, PMMA exhibited the highest echo reduction as the absorbing polymer. Interestingly, ARMS performance remained largely stable across the tested materials, with only a 6% difference in echo reduction between the worst-performing polymer (Melopas) and the best. Therefore, optimal ARMS performance can be achieved with an array pitch of 10 mm, a pillar height of 4 mm at 1 MHz, and PMMA as the absorbing polymer. The performance of the optimized ARMS is illustrated in Fig.6.

C. Comparison with conventional substrates

The performance of the optimized ARMS was compared to that of conventional substrates, including glass, PS, PDMS, and PMMA. As shown in Fig.7, the ARMS significantly reduced reflection amplitude at both Point A and Point B compared to these substrates. Compared to a glass substrate, the optimized ARMS demonstrated echo reductions of 67.2% and 86.3% at Point A and Point B, respectively. Deviation was also substantially improved, decreasing from 76.4% in glass to 19.2% in ARMS.

IV. Conclusion

This study demonstrates the potential of ARMS to significantly enhance the fidelity of *in vitro* ultrasound neuromodulation studies. We optimized the ARMS design for 1 MHz and 2 MHz ultrasound frequencies and found that the combination of

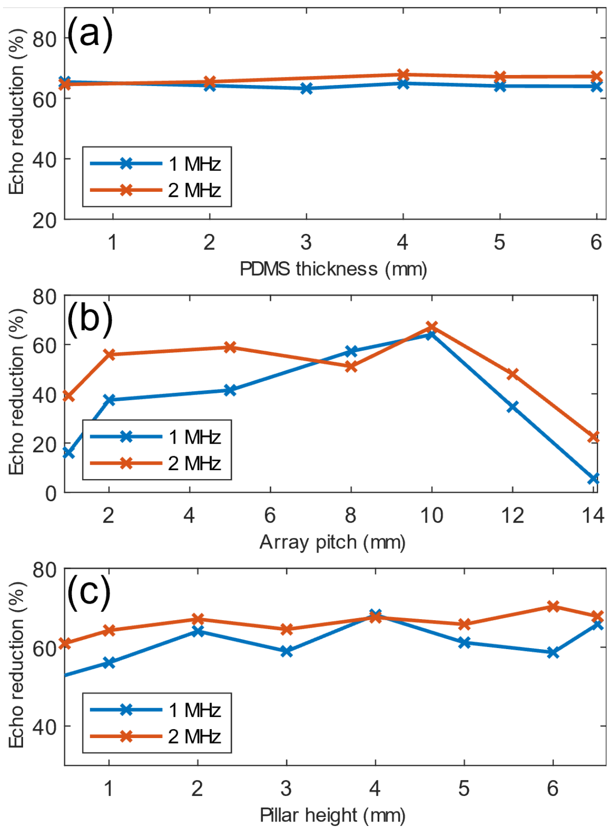

Fig. 4. Optimization of ARMS dimensions at 1 and 2 MHz frequencies: Echo reduction as a function of (a) PDMS thickness, (b) array pitch, and (c) pillar height.

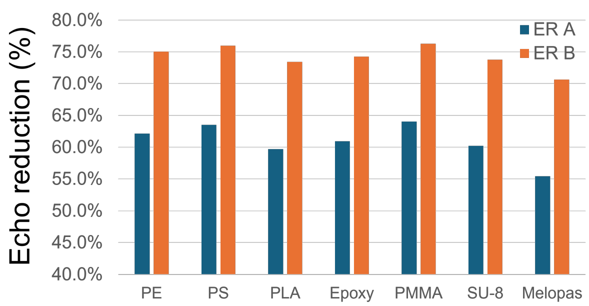

Fig. 5. The effect of different polymers as the absorbing polymer on the echo reduction of ARMS.

PDMS and PMMA yielded the best performance. We observed that ARMS performance was influenced by the array pitch and pillar height. The optimized ARMS reduced the peak-to-peak echo amplitude on the substrate surface by 86.3% compared to a glass substrate and preserved stimulation signal fidelity with a deviation of 19.2%, a marked improvement from the 76.4% deviation observed with glass. Following these promising results, we plan to experimentally validate this concept, including the use of composite polymers, which can improve the performance of ARMS but are challenging to simulate.

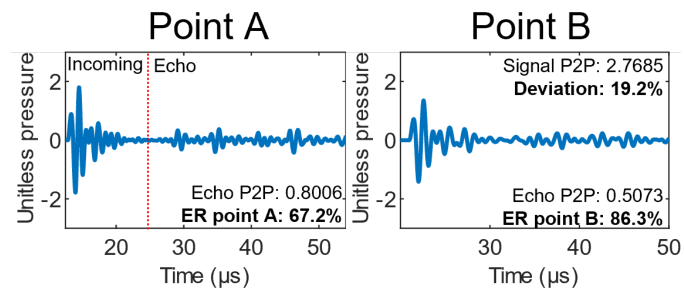

Fig. 6. The time-domain simulation result of optimized ARMS at Point A and Point B, which shows the suppression of the echo at both observation points and preservation of the primary signal fidelity at Point B.

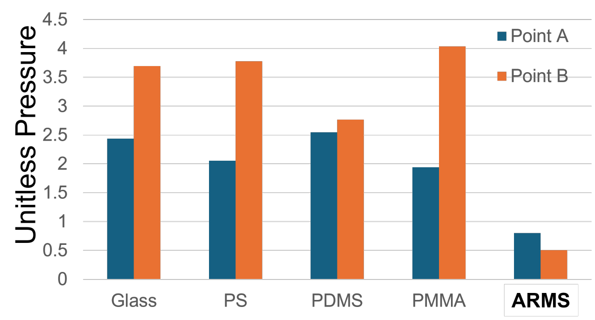

Fig. 7. Comparison of echo amplitude at Point A and B for the optimized ARMS and conventional substrates (glass, PS, PDMS, and PMMA).

References

[1] J. Blackmore et al., “Ultrasound neuromodulation: A review of results, mechanisms and safety,” Ultrasound in Medicine and Biology, vol. 45, no. 7, pp. 1732-1752, 2019.

[2] H. A. S. Kamimura et al., “Ultrasound neuromodulation: Mechanisms and the potential of multimodal stimulation for neuronal function assessment,” Frontiers in Physics, vol. 8, 2020.

[3] I. M. Suarez-Castellanos et al., “Spatio-temporal characterization of causal electrophysiological activity stimulated by single pulse focused ultrasound: An ex vivo study on hippocampal brain slices,” Journal of Neural Engineering, vol. 18, no. 2, 2021.

[4] S. Yoo et al., ”Focused ultrasound excites cortical neurons via mechanosensitive calcium accumulation and ion channel amplification,” Nature Communications, vol. 13, no. 1, pp. 368, 2022.

[5] A. R. Selfridge, “Approximate material properties in isotropic materials,” IEEE Transactions on Sonics and Ultrasonics, vol. 32, no. 3, pp. 381-394, 1985.

[6] H. Shankar and P. S. Pagel, ”Potential adverse ultrasound-related biological effects: A critical review,” Anesthesiology, vol. 115, no. 5, pp. 1109-1124, 2011.

[7] N. N. Liu, Y. D. Cui, B. C. Khoo, and A. M. Zhang, ”Damage characteristics of elastic material through a thin membrane using high-intensity focused ultrasound (HIFU),” AIP Advances, vol. 8, no. 11, pp. 115123, 2018.

[8] Y. Wang, J. Tao, F. Guo, S. Li, X. Huang, J. Dong, and W. Cao, ”Magnesium alloy matching layer for high-performance transducer applications,” Sensors (Switzerland), vol. 18, no. 12, pp. 4424, 2018.

[9] A. Ndieguene et al., ”SU-8 photoresist and SU-8 based nanocomposites for broadband acoustical matching at 1 GHz,” Journal of Physics: Conference Series, vol. 195, pp. 012005, 2009.

[10] H. Aydogmus et al., ”An organ-on-chip device with integrated charge sensors and recording microelectrodes,” Scientific Reports, vol. 13, no. 1, pp. 7901, 2023.

[11] C. J. Mandrycky et al., ”Organ-on-a-chip systems for vascular biology,” Journal of Molecular and Cellular Cardiology, vol. 159, pp. 1-13, Oct. 2021.